Electronic Supplementary Material (ESI) for New Journal of Chemistry.

Supplementary Information

Fabrication of durable self-repairing superhydrophobic fabrics via a fluorinate-free waterborne biomimetic silicification strategy

Yihan Sun[a, c] , Jinxia Huang [a] , Siyang Zhao [a, c] and Zhiguang Guo[a, b*]

[a] *State Key Laboratory of Solid Lubrication, Lanzhou Institute of Chemical Physics, Chinese Academy of Sciences, Lanzhou 730000, China.*
[b] *Hubei Collaborative Innovation Centre for Advanced Organic Chemical Materials and Ministry of Education Key Laboratory for the Green Preparation and Application of Functional Materials, Hubei University, Wuhan 430062, China*
[c] *University of Chinses Academy of Sciences, Beijing 100049, P. R. China*

**Corresponding author. Tel: 0086-931-4968105; Fax: 0086-931-8277088. Email address: zguo@licp.cas.cn (Guo)*

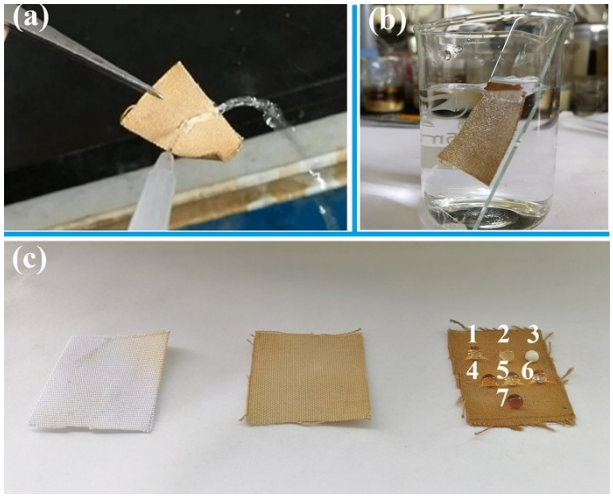

Fig. S1. The excellent water resistance performance of the obtained superhydrophobic fabric. (a) A jet of water can bounce off the test samples. (b) A silver mirror-like phenomenon occurred when a fabric attached to a glass slide was soaked in water. (c) Seven kinds of liquid droplets can spread on pristine cotton fabric (left) and pristine cotton fabric @ TA-APTES (middle), while they can remain marble-like on pristine cotton fabric @ TA-APTES-ODA (right). The aqua-phase liquid 1,2,3,4,5,6 and 7 is water, juice, milk, coke cola, Sprite, green tea and coffee, respectively.

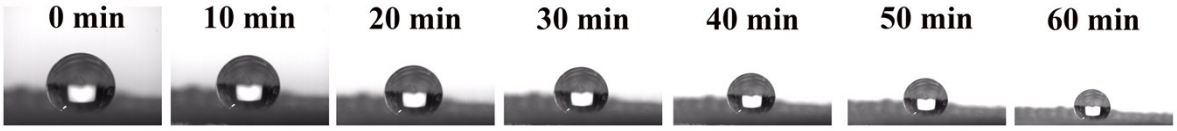

Fig. S2. Water droplets on the obtained superhydrophobic fabric for different time periods.

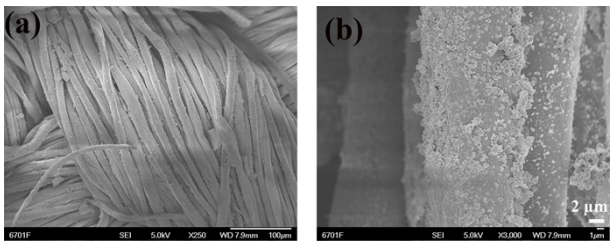

Fig. S3. The SEM images of backside of the obtained superhydrophobic fabric.

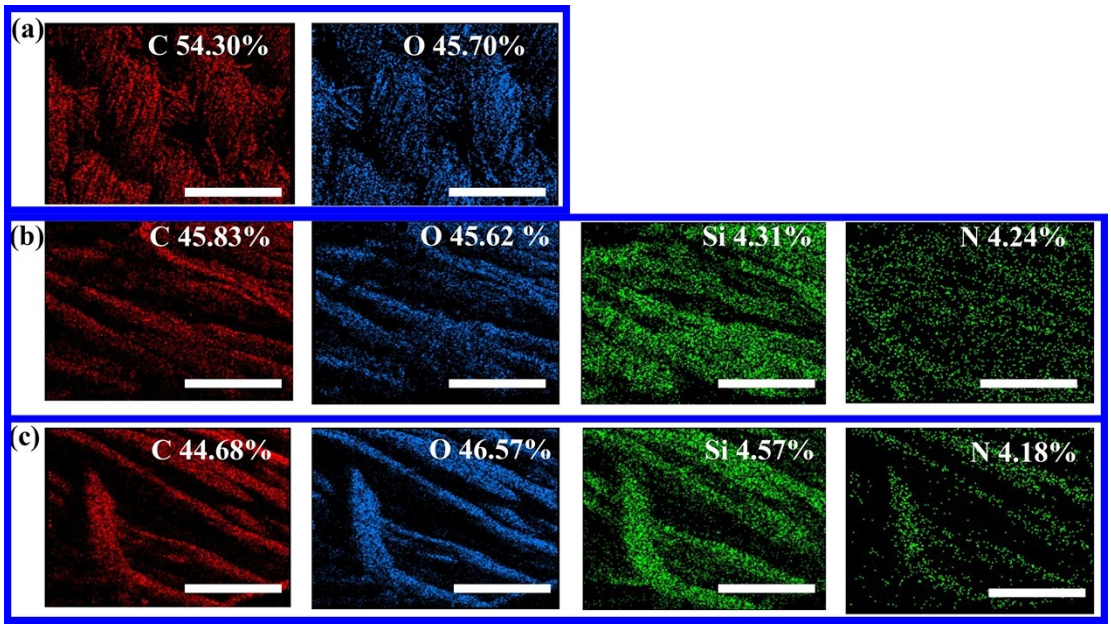

Fig. S4. The EDS mapping and element weight ratio of the pristine cotton fabric (a), pristine cotton fabric @ TA-APTES and pristine cotton fabric @ TA-APTES-ODA. The scar bar is 100 μm.

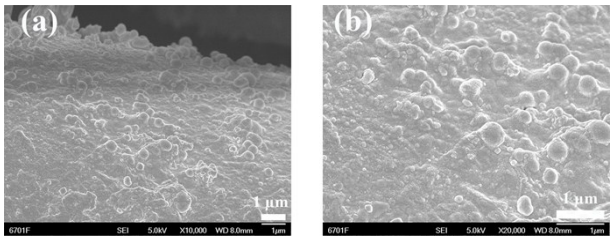

Fig. S5. The magnitude SEM images of the obtained superhydrophobic fabric.

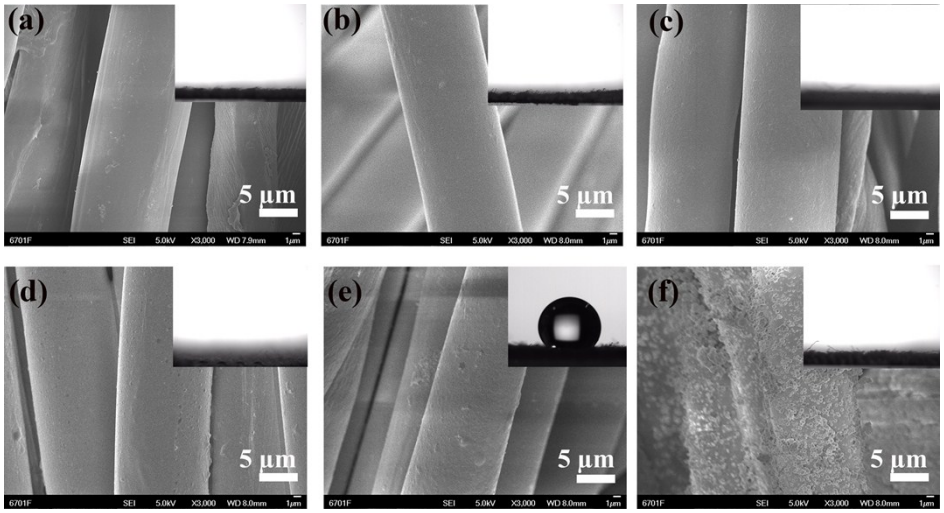

Fig. S6. The SEM images of cotton fabric treated with TA (a), APTES (b), ODA (c), APTES +ODA (d), TA +ODA (e), and TA +APTES (f). The insets are water contact angles on each treated fabric.

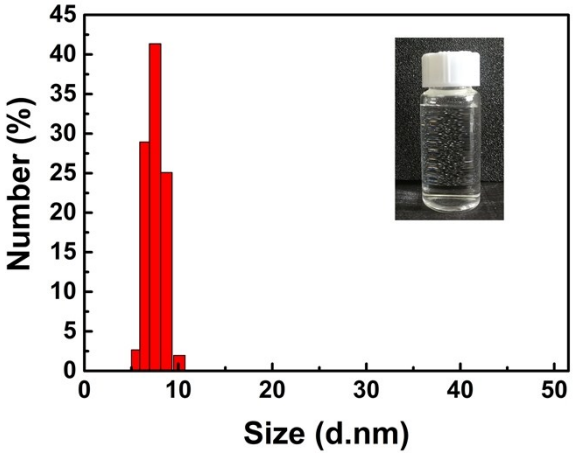

Fig. S7. The dynamic light scattering (DLS) result of the sole APTES without TA in solution. The inset is the optical photography of the coating solution of sole APTES.

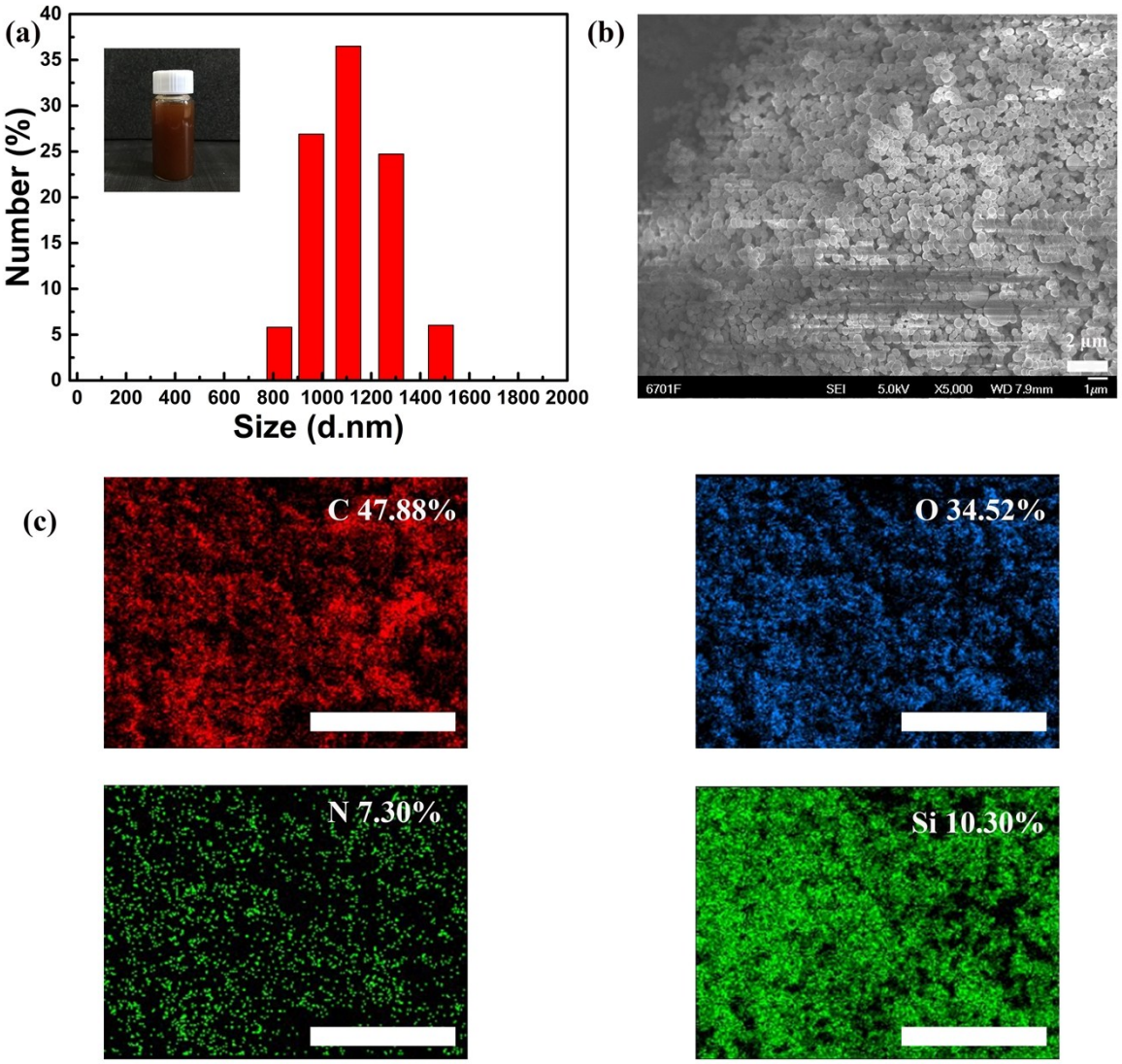

Fig. S8. (a) The size distribution of colloid nanoparticles in the TA-APTES coating solution after 12h. The inset is the optical photography of the TA-APTES solution. (b) The SEM image of nanoparticles in the TA-APTES solution. (c) The EDS mapping of the formed colloid nanoparticles. The scar bar is 100 μm.

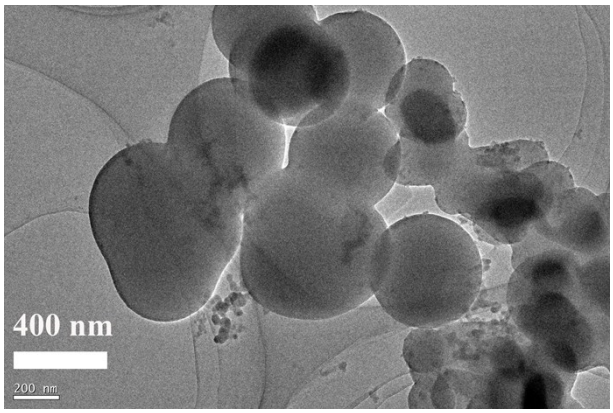

Fig. S9. TEM images of formed amino group-terminated silica nanoparticles in TA-APTES solution after 12 h.

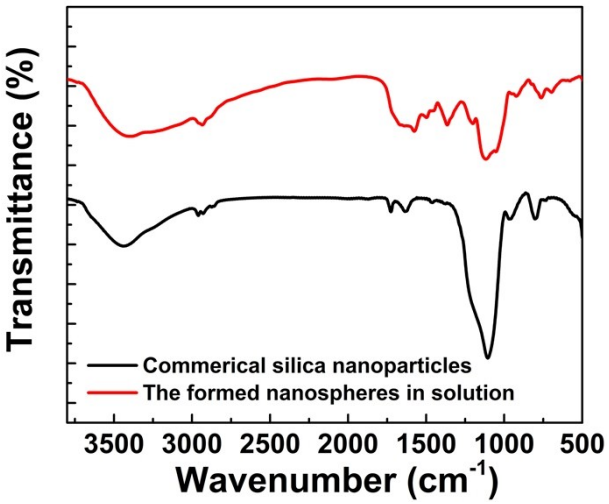

Fig. S10. The FTIR spectra of the commercial silica nanoparticles and the formed nanoparticles in the TA-APTES solution after 12 h.

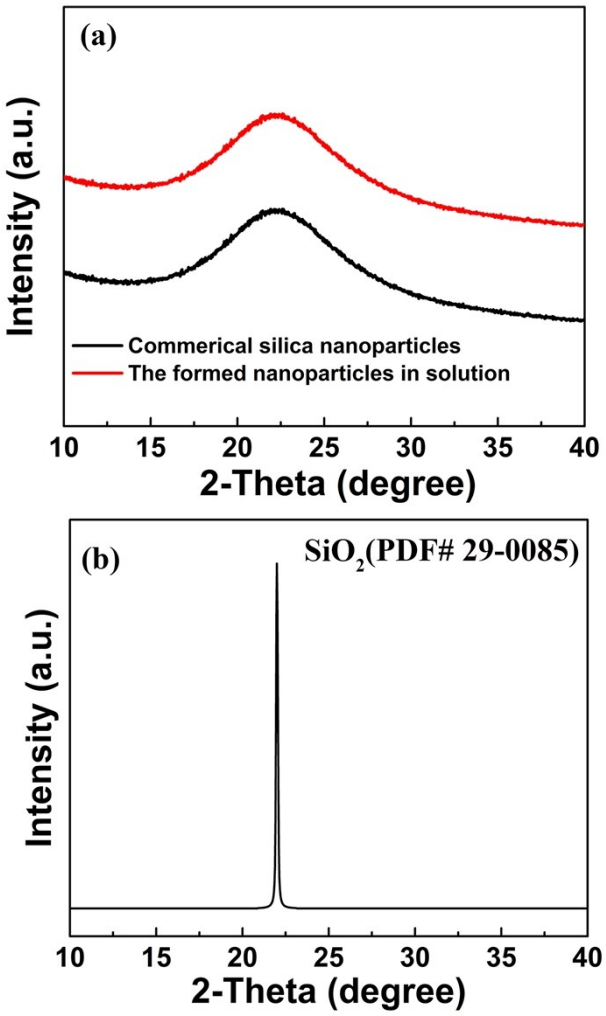

Fig. S11. (a) The XRD patterns of commercial silica nanoparticles and the formed nanoparticles in the TA-APTES solution after 12 h. (b) The standard XRD PDF card of silica.

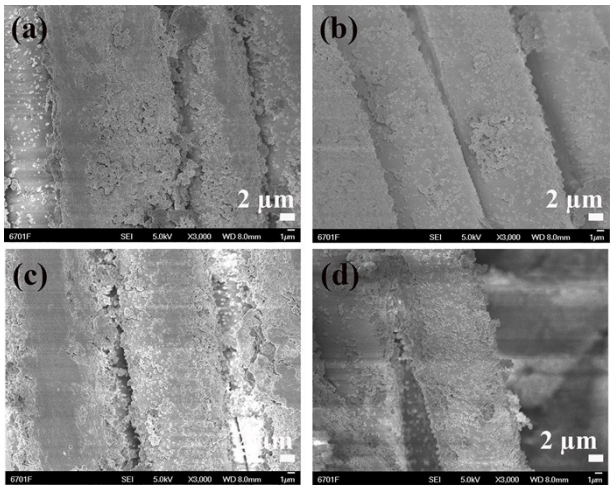

Fig. S12. The SEM images of treated superhydrophobic fabric after being soaked in ethanol (a), n-hexane (b), xylene (c) and acetone (d) after 24h at temperature, respectively.

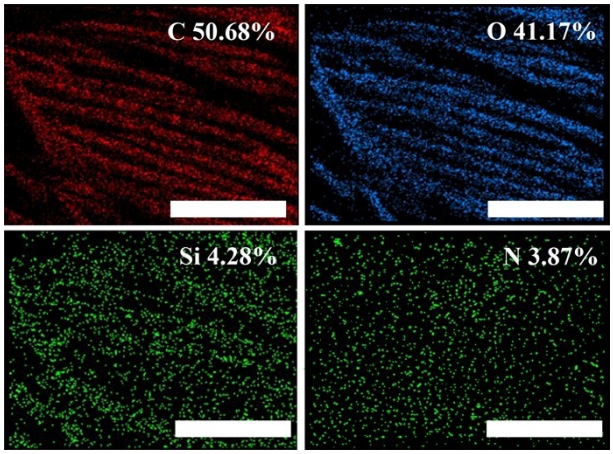

Fig. S13. The EDS mapping of the obtained superhydrophobic fabric after 20 times of washing cycles. The scar bar is 100 µm.

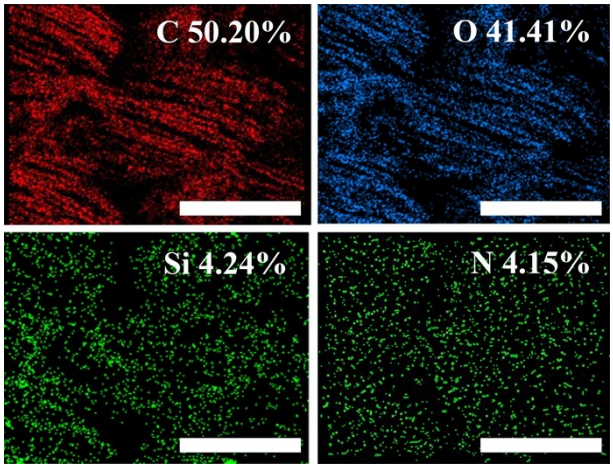

Fig. S14. The EDS mapping of the obtained superhydrophobic fabric after 50 times of abrasion cycles. The scar bar is 100 μm.

Fig. S15. The optical photographs of pristine cotton fabric, pristine cotton fabric @ TA-APTES and pristine cotton fabric @ TA-APTES-ODA after being soaked into the water dyeing with methyl blue. The superhydrophobic fabric shows excellent anti-fouling behavior.

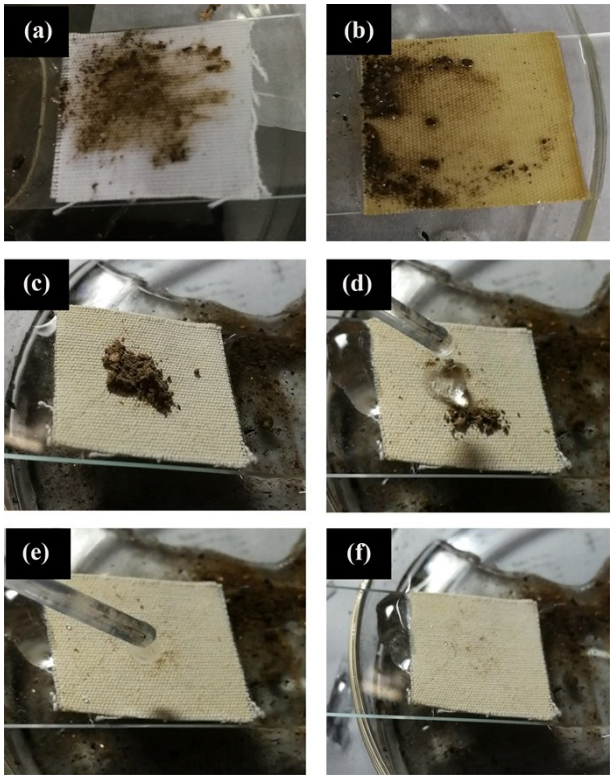

Fig. S16. The self-cleaning behavior of the pristine cotton fabric (a), pristine cotton fabric @ TA-APTES (b) and pristine cotton fabric @ TA-APTES-ODA (c-f) with a layer of dust particles.

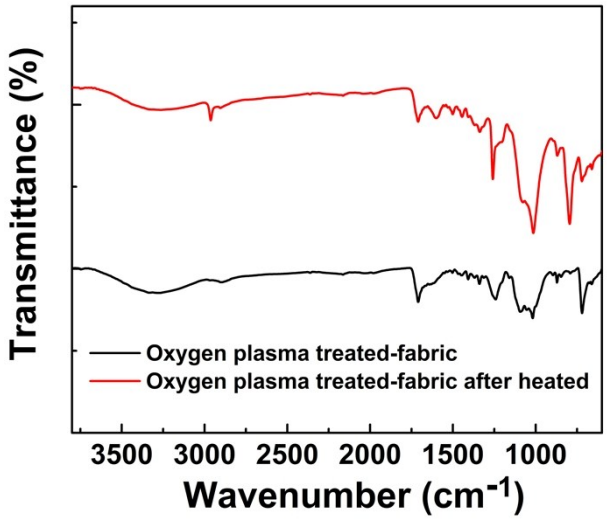

Fig. S17. The FTIR spectra of oxygen plasma treated-fabric and oxygen plasma treated fabric after heat treatment.

Fig. S18. The optical photographs of water on dyed fabric with self-healing function.

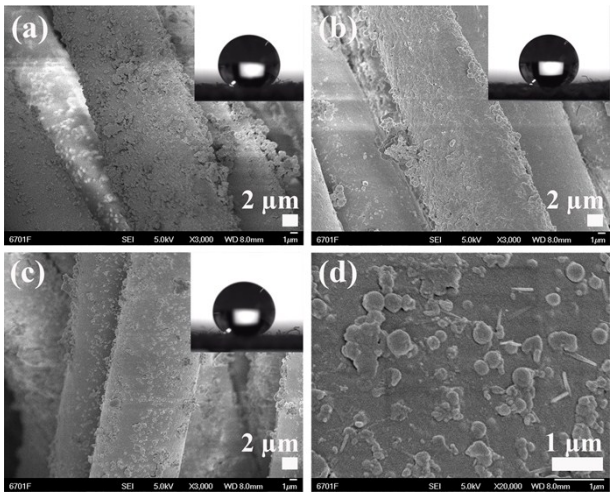

Fig. S19. The SEM images and contact angles of dyed self-healing fabrics after heated. (a) The fabric dyed with blue color. (b) The fabric dyed with yellow color. (c-d) The fabric dyed with red color.

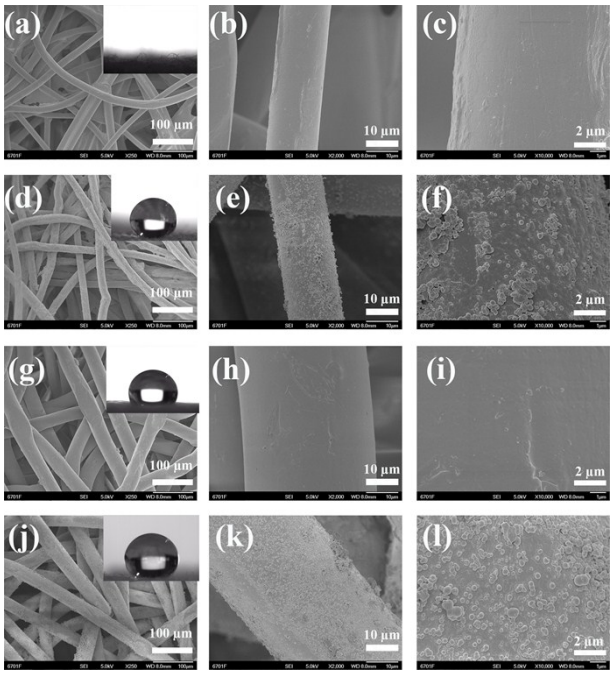

Fig. S20. The SEM images of pristine PET polyester fabric (a-c), superhydrophobic PET fabric (d-f), pristine PP unwoven fabric (g-i) and superhydrophobic PP fabric. The inset in (a), (d), (g) and (j) is the water contact angle of the pristine PET fabric, superhydrophobic PET fabric, pristine PP fabric and superhydrophobic PP fabric, respectively.

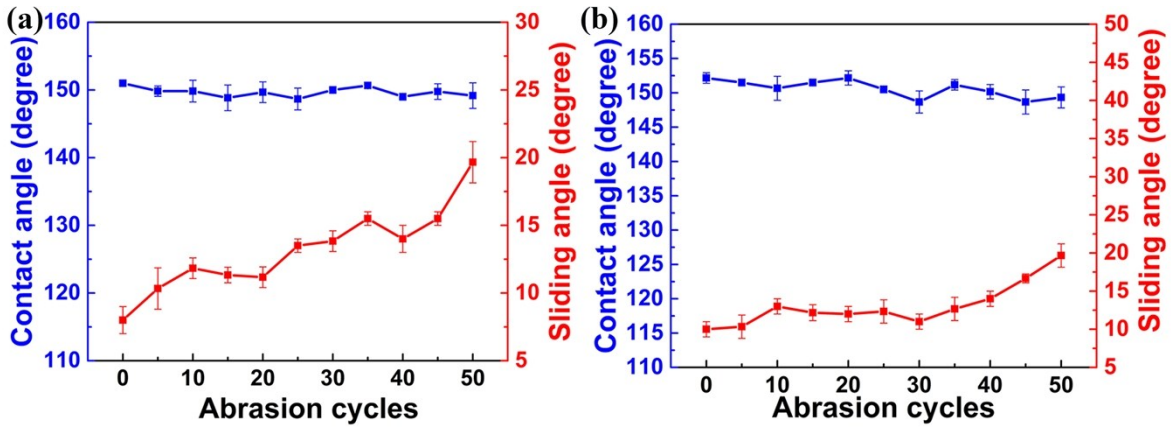

Fig. S21. The water contact angle and sliding angle with abrasion cycles of the treated PET fabric (a) and PP fabric (b).

References

1 Z. Wang, S. Ji, F. He, M. Cao, S. Peng and Y. Li, *J. Mater. Chem. A.*, 2018, **6**, 3391-3396.

2 Z. Wang, S. Ji, J. Zhang, F. He, Z. Xu, S. Peng and Y. Li, *J. Membr. Sci.*, 2018, **564**, 317-327.

3 S. Liu, H. Zhou, H. Wang, W. Yang, H. Shao, S. Fu, Y. Zhao, D. Liu, Z. Feng and T. Lin, *Small,* 2017,**13**,1701891.

4 S. Gu, L. Yang, W. Huang, Y. Bu, D. Chen, J. Huang, Y. Zhou and W. Xu, *Cellulose*, 2017, **24**, 2635-2646.

5 Y. Z. Zhu, F. Zhang, D. Wang, X. F. Pei, W. B. Zhang and J. Jin, *J. Mater. Chem. A.*, 2013, **1**, 5758-5765.

6 S. J. Gao, Y. Z. Zhu, F. Zhang and J. Jin, *J. Mater. Chem. A.*, 2015, **3**, 2895-2902.